

1433. A wavelet-based algorithm for numerical integration on vibration acceleration measurement data

Dishan Huang¹, Jicheng Du², Lin Zhang³, Dan Zhao⁴, Lei Deng⁵, Youmei Chen⁶

^{1,2,3}School of Mechatronic Engineering and Automation, Shanghai University, Shanghai, China

^{4,5,6}Shanghai Engineering Center of Microsatellites, Shanghai, China

¹Corresponding author

E-mail: ¹hdishan@shu.edu.cn, ²djicheng123@163.com, ³zhanglin123581@hotmail.com,

⁴zhaodan_hit@yahoo.com.cn, ⁵denglei@mail.sim.ac.cn, ⁶amei1017@sina.com

(Received 20 January 2013; received in revised form 10 September 2014; accepted 13 October 2014)

Abstract. This paper will present a wavelet-based algorithm for numerical integration. The contribution of the manuscript is that: 1) Define an integration wavelet, which is applied to the numerical integration and applicable for processing stationary vibration data; 2) The basic properties of integration wavelet, such as frequency response, convolution solution with zero mean, stability and ripple in pass-band are discussed, and the investigation results reveal the excellent properties of it; 3) The validity of presented approach is illustrated by numerical integration computation on angular oscillation of a pendulum. The theoretical research and engineering experiments show that the presented approach is valuable in the vibration signal estimation.

Keywords: integration wavelet, numerical integration, vibration signal estimation.

1. Introduction

As known, acceleration, velocity and displacement are regular physical measurements of vibration testing. Study the transformation among them is often encountered in many engineering problems. However, due to initial value, noise [1] and drift, a simple numerical integration algorithm is usually unstable for the engineering problem. Until now, the double integration real time processing on vibration acceleration signal were realized on hardware-based integrator in some vibration test.

Now, the new method of numerical integration is being studied for converting a measured history of acceleration data into a displacement data. There are two types of algorithm developed. One is by integrating the acceleration signal in the time domain. The typical case is an adaptive algorithm combined with band-limited multiple Fourier linear combiners (BMFLC) which can eliminate the problem of drifting in the numerical integration [2]. The other is by dividing the Fourier-transformed acceleration signal by the scale factor of $-\omega^2$ and taking its inverse Fourier transform, such as an improved frequency domain method used in the reconstruct displacement signal from a measured acceleration response [3].

However, in recent years, the wavelet-based algorithm has been paid attention in integration numerical computation [4-6]. It can be applicable in the context of numerical approximation of integral equations, partial differential equations, ordinary differential equations [7-9] and signal identification [10]. Unfortunately, for unknown mathematic model and initial conditions for the vibration data in the engineering application, the given wavelet based algorithm in the literature [4-9] could not be directly employed in the vibration data estimation.

To solve the problem of numerical integration for vibration acceleration, the following work is done in this paper; 1) an integration wavelet is defined; 2) the numerical integration can be realized by the integration wavelet convoluting with the discrete time vibration signal; 3) the important properties of integration wavelet are discussed, and an experiment is given to demonstrate the validity and applicability of this new approach.

2. Combination wavelet

Consider a mother wavelet $h(t)$ as a combination wavelet, and it is mathematically described in the combination of a series of harmonic components with a window [13]:

$$h(t) = W(t) \sum_{i=L}^H \cos(2\pi f_i t), \tag{1}$$

where $W(t)$ is a window, f_L and f_H are start frequency and cut-off frequency respectively. $W(t)$ is introduced for cut down the ripple in pass-band of the frequency response $h(f)$.

$h(t)$ can be regarded as the linear superposition of $(H-L)$ wavelets. The Fourier transform pair of the combination wavelet $h(t)$ is that:

$$W(t) \sum_{i=L}^H \cos(2\pi f_i t) \Leftrightarrow W(f) * \left(\sum_{i=L}^H \delta(f - f_i) + \sum_{i=L}^H \delta(f + f_i) \right). \tag{2}$$

$h(t)$ can mathematically be explained a convolution result of a gate function with a window in the frequency domain while the frequency increment from f_L to f_H is set to 1. The wavelet $h(t)$ is a pass-band filter with linear phase because of several cosine waves combination. The frequency response characteristic of the combination wavelet is shown in Fig. 1, it is obvious that the linear superposition of equal space wavelets is the foundation of filter with bandwidth. On the condition of limitation, the frequency response range of the combination wavelet can be expanded from $f_L = 1$ to $f_H = N/2$, and the excellent frequency response characteristic has been constructed.

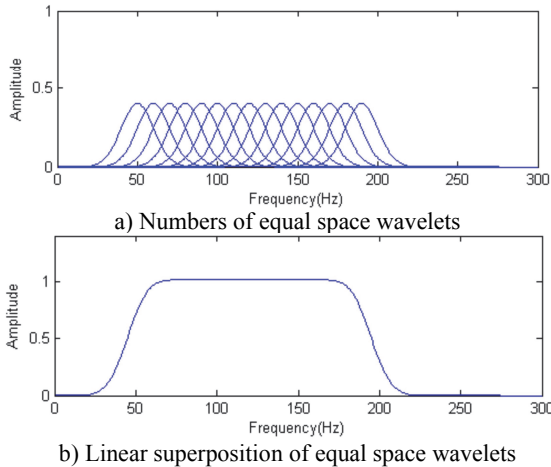


Fig. 1. Schematic of a combination wavelet construction

3. Integration wavelet

Based on the combination wavelet in the Eq. (1), introduce an integration operation on it:

$$h_g(t) = W(t) \int \sum_{i=L}^H \cos(2\pi f_i t) dt = W(t) \sum_{i=L}^H \frac{\sin(2\pi f_i t)}{2\pi f_i}. \tag{3}$$

Let $f_L = 1$ and $f_H = N/2$, the frequency increment be 1. Then, $h_g(t)$ is defined as an integration wavelet. The range of frequency response of integration wavelet covers from 1 to $N/2$.

As stated as the above section, the action of window $W(t)$ is to decay the pass-band ripple in the frequency response of integration wavelet.

As shown in Fig. 2, that is a waveform of a discrete integration wavelet. The length of this integration wavelet $N = 3679$, the start frequency $f_L = 1$, the cut-off frequency $f_H = 1839$, and the frequency increment 1. $W(t)$ is the Kaiser window [6] which is a one parameter family of window functions, where the parameter $\beta = 1$. The frequency response of integration wavelet $h_g(t)$ is shown in Fig. 3, and it approaches to the one of an ideal integrator.

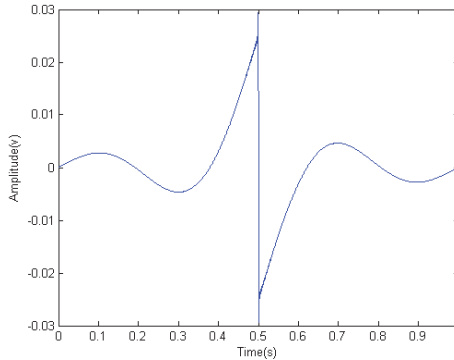


Fig. 2. Waveform of integration wavelet $h_g(t)$
 (The length of integration wavelet $N = 3679$, $f_L = 1$ and $f_H = 1839$)

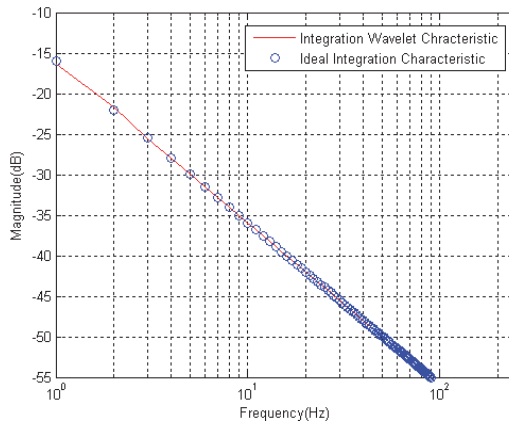


Fig. 3. Frequency response of integration wavelet

4. Numerical integration

Because of the integration characteristic of the presented integration wavelet, when the integration wavelet $h_g(t)$ convolutes with a vibration signal $x(t)$, the integration operation can be realized, and it is expressed as:

$$y(\tau) = \int_0^{\tau} x(t)h_g(t - \tau)dt. \quad (4)$$

The numerical integration is done in the time domain through convoluting the integration wavelet with a time series.

In practice, the digital integration wavelet $h_g(n)$ convolutes with a vibration acceleration measurement data $a(n)$, the estimation of vibration velocity $v(n)$ can be obtained in the time

domain. If one more convolution operation is carried out, the estimation of vibration displacement $d(n)$ will be realized.

5. Characteristics of integration wavelet

5.1. Frequency response

The parameter β in the Kaiser window will affect the frequency response characteristic of the integration wavelet. When β increases, the frequency response attenuates in the range of low frequency. The detail issue is illustrated in the frequency characteristics shown in Fig. 4. It is obvious that the attenuation happens in the frequency range of less than 2 Hz.

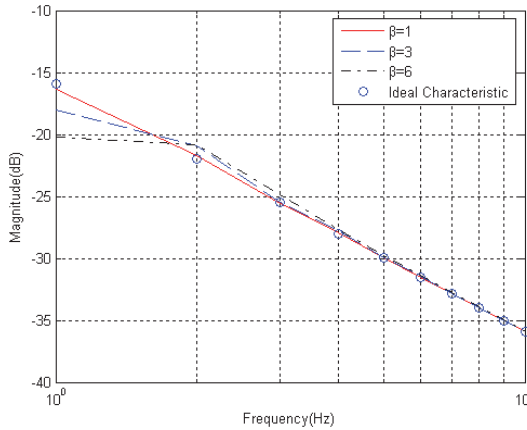


Fig. 4. The parameter β in the Kaiser window affects the frequency response of an integration wavelet

5.2. Zero-mean and stability

Based on Eq. (3), the sine wave is selected in the construction of an integration wavelet, and the point of discrete time waveform is selected as odd number. Thus, the integration wavelet is an odd function, and the convolution operation on measurement data can remove the direct component. Therefore, the numerical integration is replaced by wavelet convolution operation, which is applicable for processing on a stationary acceleration signal. The advantages of wavelet-based integral algorithm as follows:

- No disturbance of initial value on numerical integration;
- Numerical integration result without direct component or tendency.

In additional, the integration wavelet is FIR construction, therefore, it is a kind of stable digital filter. Though the presented algorithm makes the computation loads little bit high in the application, the numerical integration on a time series will be stable.

5.3. Ripple in pass-band

When the integration wavelet convolutes with signal, the ripple in pass-band impliedly exists in the convolution result. In specially, the serious ripple will occur in the frequency around f_L . If the convoluted signal with non-integer period, the ripple in pass-band will be remarkable in the convolution result. However, as the parameter β increases in the Kaiser window, the ripple in pass-band will be decayed in the band edge. The effect of parameter β in the Kaiser window on the ripple in pass-band is shown in Fig. 5, where the length of wavelet is 257, and the frequency parameter $f_L = 1$.

As motioned above, the quality of frequency response and the ripple in pass-band are dependent on selection of parameter β in the Kaiser window. However, the selection of parameter

β is ambivalent for them. Therefore, it needs to balance the quality of frequency response and the ripple in pass-band in the selection of parameter dimension of the Kaiser window. In fact, β is selected in the range of 1-4, both of the attenuation in the frequency response at $f_L = 1$ and the ripple in pass-band can be controlled in less than 30 % (-3 dB).

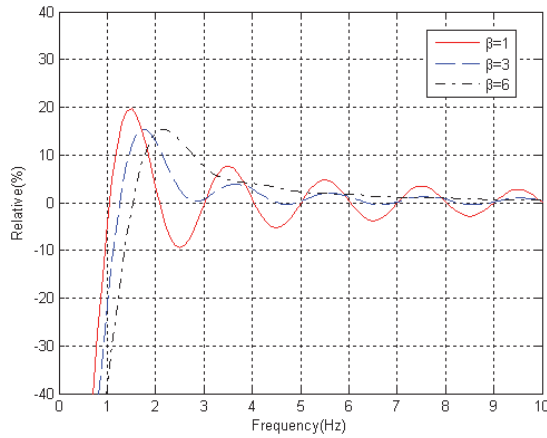
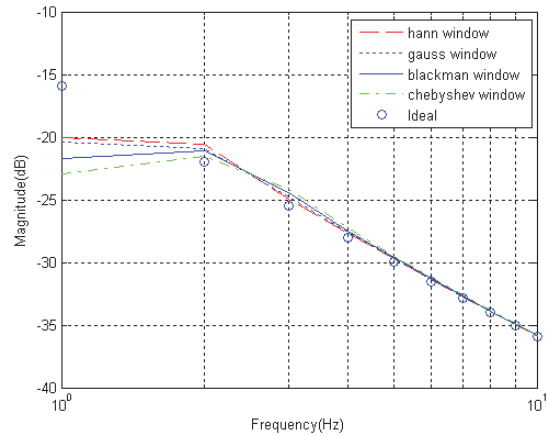
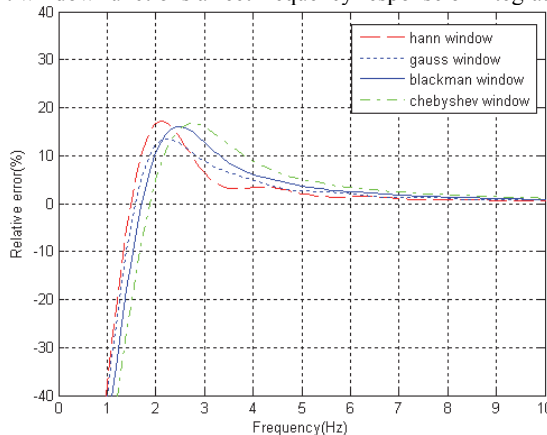


Fig. 5. Parameter β in the Kaiser window affects pass-band ripple



a) Different window functions affect frequency response of integration wavelet



b) Different windows affect ripple in pass-band

Fig. 6. Different windows affect frequency response of integration wavelet

5.4. Window function

Many window functions can be selected to construct the wavelet. The type of window will significantly influence the frequency response. Thus, it is necessary to observe the Kaiser window in comparison with the other window.

As shown in Fig. 6(a), the frequency responses in the range of lower frequency is sensitive to selection of window. It is obvious that the effect of Hanning, Gauss, Blackman and Chebyshev window on the frequency response characteristics are worse than Kaiser window ($\beta = 1-3$).

The ripple in pass-band is also related to the selection of window. As shown in Fig. 6(b), although Hanning, Gauss, Blackman and Chebyshev window can improve the ripple in pass-band around frequency $f_L = 1$, the attenuation in the frequency response edge is still beyond 3 dB.

6. Example

An example is given to illustrate the superiority of the presented approach over existing techniques. A discrete time acceleration data is expressed as: $x(n) = A\sin(2\pi fn)$, where $A = 1$ and $f = 400$ Hz and $n = 1, 2, 3, \dots$, and the waveform is shown in Fig. 7. The result of two integrations realized by the presented integration wavelet is shown in Fig. 8. In contrast to integration performance, as shown in Fig. 9, the two integrations are directly done by the algorithm of numeric integration. It is obvious that there are a non-zero-mean value in an integral and a tendency in double integral because of unknown initial condition in the original algorithm, which is not adapted to process the problem of stationary vibration measurement data. However, the presented approach can overcome all defeats caused by the original algorithm of numerical integration.

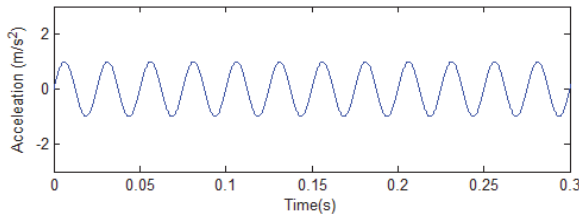
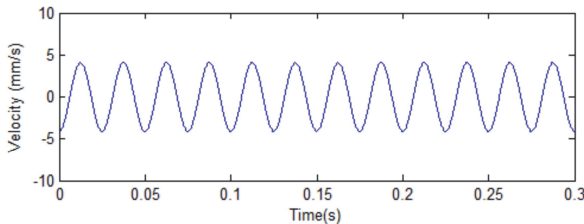
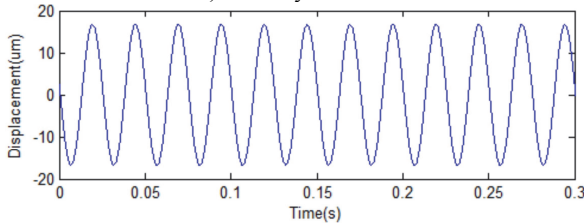


Fig. 7. A sinusoidal data $x(n) = A\sin(2\pi fn)$, where $A = 1$ and $f = 400$ Hz



a) Velocity estimation



b) Displacement estimation

Fig. 8. Result of two integrations realized by the presented integration wavelet

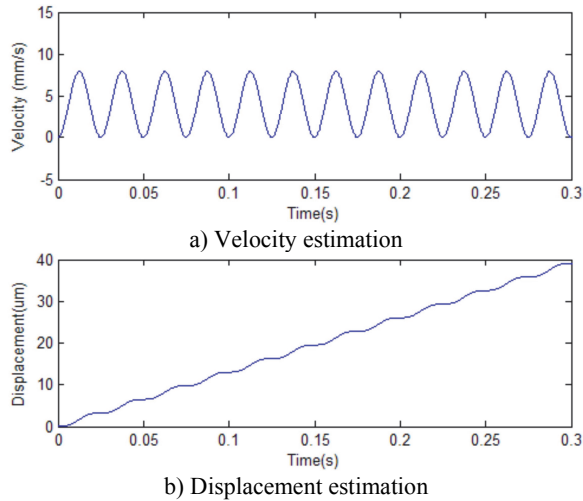


Fig. 9. Result of two integrations realized by algorithm of numerical integration

7. Application of signal detection

An application is to compare the angular oscillation wave estimation by the presented integration wavelet processing with a laser measured result. Fig. 10 is a schematic of angular oscillation detection with two accelerometers. Angular acceleration α is measured from these two accelerometers on the rod pendulum. The angular acceleration α is expressed as the form of signal combination:

$$\alpha = \frac{a_1 - a_2}{d} \tag{5}$$

The angular displacement θ_1 is estimated by:

$$\theta_1 = \iint \alpha dt dt \tag{6}$$

The double integrations are realized by applying the presented integration wavelet.

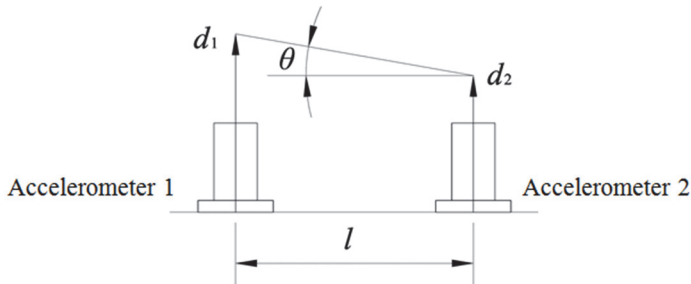


Fig. 10. Principle of displacement estimation with two accelerometers

Fig. 11 is a scheme of measurement system of angular oscillation, and Fig. 12 is a photo of angular oscillation measurement. A sine signal from a signal generator is sent to a power amplifier (YE5871A), and drives a shaker (JZK-2) to excite the rod pendulum. Then the rod pendulum oscillates, and two accelerometers (CA-YD-186) pick up the acceleration signals at different locations. After data acquisition (ECON: MI-8008), the signal combination and numerical integration are processed by the presented approach. At the same time, a laser displacement sensor

(Keyence: LK-G10, Resolution: 0.01 μm) gets the displacement of the end of rod, which is used to calibrate the angular oscillation. The angular displacement θ_2 obtained by the laser measurement can be expressed as:

$$\theta_2 = \frac{s}{l}, \tag{7}$$

where s is vibration displacement obtained by the laser, and l is effective length from the detecting point to the rotating point.

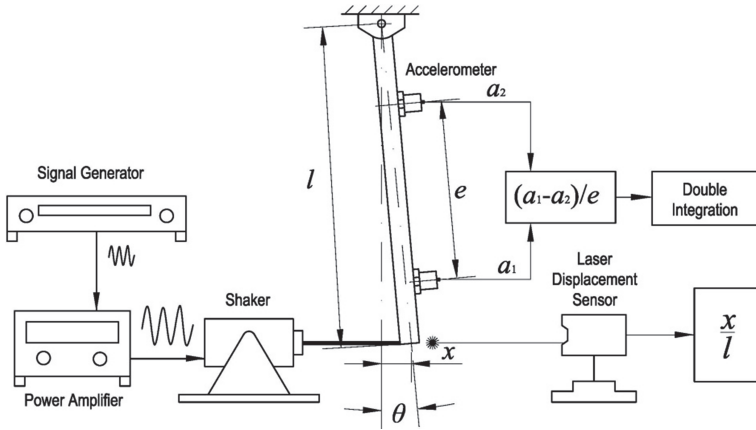


Fig. 11. Schematic of angular oscillation measurement

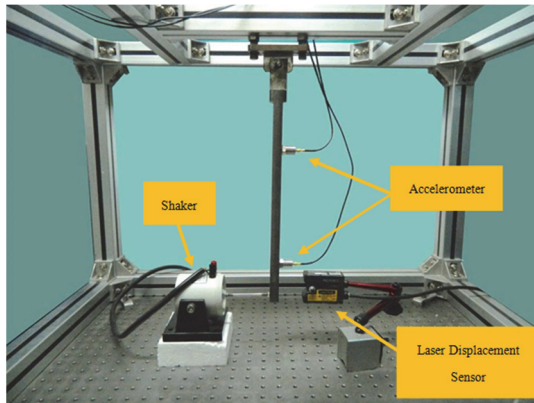


Fig. 12. Photo of angular oscillation measurement

The angular oscillation is estimated by the integration wavelet convoluting with the angular acceleration signal, and the estimated result is illustrated in Fig. 13. The exciting frequency is 10 Hz in the vibration test. The RMS value of the angular oscillation wave obtained by the integration wavelet is 54.29 μrad , and another one measured by the laser displacement sensor is 54.41 μrad . The difference between them is about 0.22 %. The measured result by the presented method is highly agreement with the one by the laser measurement.

The presented approach was used to detect an angular oscillation of the optical payload in a satellite ground test, and the angular oscillation measurement data and its spectrum are shown in Fig. 14. The oscillation source of the optical payload came from a momentum wheel installed in the satellite body. The measurement result was used to assess the influence of the momentum wheel on the payload. The time series was obtained by double integrals on an angular acceleration oscillation off-line. The presented numerical integration can attain the angular measurement

resolution less than $1 \mu\text{rad}$ in the engineering application. Besides, the problem of initial value is no longer to disturb the estimation of angular oscillation.

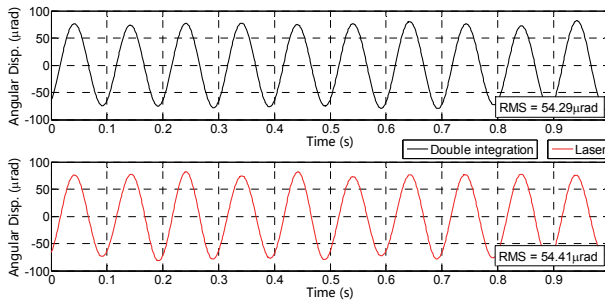


Fig. 13. Angular acceleration measured by combination result of twin sensors

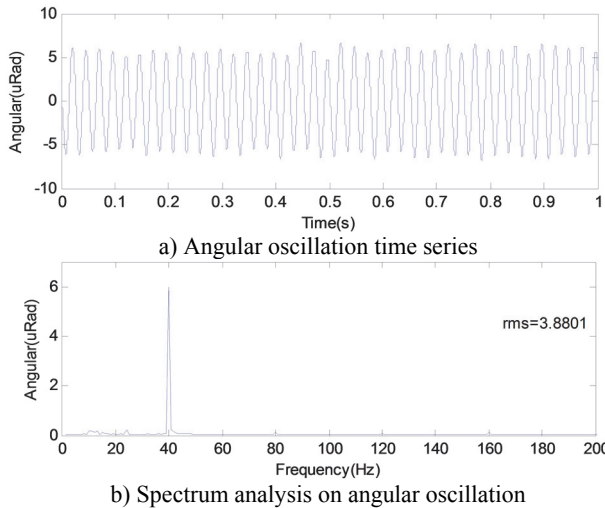


Fig. 14. Angular displacement estimation on optical load in a satellite

8. Conclusions

Based on a combination wavelet, an integration wavelet is defined, and it is used in the numerical integration adapted for processing a stationary vibration data. The estimations of vibration velocity and displacement are realized by convoluting the integration wavelet with a vibration acceleration data. The advantage of the presented integration wavelet is of high accuracy and good stability in the numerical integration operation on the condition of unknown initial condition. So it is recommended to be used in the numerical integration of stationary vibration acceleration measurement data.

References

- [1] **Thong Y. K., et al.** Numerical double integration of acceleration measurements in noise. *Measurement*, Vol. 36, 2004, p. 43-92.
- [2] **U-Xuan Tan, et al.** Estimation displacement of periodic motion with inertial sensor. *IEEE Sensors Journal*, Vol. 8, Issue 8, 2008, p. 1385-1388.
- [3] **Sangbo Han** Measuring displacement signal with an accelerometer. *Journal of Mechanical Science and Technology*, Vol. 24, Issue 6, 2010, p. 1329-1335.

- [4] **Babolian E., Fattahzadeh F.** Numerical computation method in solving integral equations by using Chebyshev wavelet operational matrix of integration. *Applied Mathematics and Computation*, Vol. 188, Issue 1, 2007, p. 1016-1022.
- [5] **Hashish H., Behiry S. H., El-Shamy N. A.** Numerical integration using wavelets. *Applied Mathematics and Computation*, Vol. 211, Issue 2, 2009, p. 480-487.
- [6] **Siraj-ul-Islam, Imran Aziz, Fazal Haq** A comparative study of numerical integration based on Haar wavelets and hybrid functions. *Computers and Mathematics with Applications*, Vol. 59, Issue 6, 2010, p. 2026-2036.
- [7] **Lepik U.** Numerical solution of evolution equations by the Haar wavelet method. *Journal of Applied Mathematics and Computing*, Vol. 185, 2007, p. 695-704.
- [8] **Hariharan G., Kannan K.** A comparative study of a haar wavelet method and a restrictive Taylor's series method for solving convection-diffusion equations. *International Journal for Computational Methods in Engineering Science and Mechanics*, Vol. 11, Issue 4, 2010, p. 173-184.
- [9] **Hariharan G., Kannan K., Sharma K. R.** Haar wavelet method for solving Fisher's equation. *Applied Mathematics and Computation*, Vol. 211, 2009, p. 284-292.
- [10] **Hariharan G., Kannan K., Kal Renganathan Sharma** Haar wavelet in estimating depth profile of soil temperature. *Applied Mathematics and Computation*, Vol. 210, 2009, p. 119-125.
- [11] **Cohen A.** Wavelets in Numerical Analysis. *The Handbook of Numerical Analysis*, Vol. VII, Elsevier, Amsterdam, 1999.
- [12] **Huang D.** A Wavelet-based algorithm for the Hilbert transform. *Mechanical System and Signal Processing*, Vol. 10, Issue 2, 1996, p. 125-134.
- [13] **Kaiser J. F.** *Digital Filters*. New York, Wiley, 1966.



Dishan Huang received Ph.D. degree in Dept. of Mechanical Engineering in Zhejiang University, Hangzhou, China in 1992. Now he teaches course of vibration and mechanical design, and does research work as an associate professor in Shanghai University. His current research focuses on the response approach of vibration and signal processing.



Jicheng Du received Master degree in School of Mechatronic Engineering and Automation of Shanghai University, Shanghai, China in 2013. Now he works at SAIC Motor Commercial Vehicle Technical Center. His current research focuses on NVH control of vehicle.



Lin Zhang received Bachelor degree in School of Mechatronic Engineering and Automation of Shanghai University, Shanghai, China in 2010. Now she works at Shanghai Huizhong Automotive Manufacturing Co. Ltd. Her current research focuses on NVH control of vehicle.



Dan Zhao received the B.S. degree in microelectronics engineering from Harbin Institute of Technology, Harbin, China, in 2005, and her Ph.D. degrees in information and communication engineering from the same university in 2010. Now she does research work as an associate researcher in Shanghai Engineering Center for Microsatellites. Her current research focuses on on-board electronics system and signal processing.



Lei Deng received the B.S. degree in electronic engineering from Zhejiang University, Hangzhou, China, in 1998, and his Ph.D. degree in physical electronics from Shanghai Institute of Technical and Physics, Chinese Academy of Science, Shanghai, China, in 2006. Now he does research work as associate researcher in Shanghai Engineering Center for Microsatellite, Shanghai, China. His current research focuses on science satellite system design, electro optical technology and image processing.



Youmei Chen received the B.S. degree in Mechanical Engineering from Hefei University of Technology, Hefei, China, in 2002, and her M.S. degree in Precision Instrument and Machinery from University of Science and Technology of China in 2007. Now, she works in Shanghai Engineering Center of Microsatellites. Her current research work focuses on structure design, jitter analysis and vibration analysis of spacecraft.